Highlights

- We have examined the long-term characteristics of EEG functional brain networks and their correlations to seizure onset
- We show periodicities over multiple time scales in network summative properties (degree, efficiency, clustering coefficient)
- We also show that, in addition to average network properties, the same periodicities exist in network topology using a novel measure (graph edit distance), suggesting that specific connectivity patterns recur over time
- These periodic patterns were preserved when we corrected for the effects of volume conduction and were found to be of much larger magnitude compared to seizure-induced modulations
- For the first time to our knowledge, we demonstrate that seizure onset occurs preferentially at specific phases of the network periodic components, particularly for shorter periodicities (around 3 and 5 hours)
- These correlations were nearly absent when examining univariate properties (EEG signal power), suggesting that network-based measures rather than EEG signal-based measures are more tightly coupled with seizure onset
- Our findings suggest that seizure detection and prediction algorithms may benefit significantly by taking into account these longer-term variations in brain network properties
- As we show strong evidence that shorter network-based periodicities (3-5 hours) are tightly coupled with seizure onset, our results pave the way for further investigation into the pathophysiology of seizure generation mechanisms beyond the well-known effects of circadian rhythms

Full-length Original Article

Multi-scale periodicities in the functional brain networks of patients with epilepsy and their effect on seizure detection

Manolis Christodoulakis*, Maria Anastasiadou*, Eleftherios S. Papathanasiou, Savvas S. Papacostas, Avgis Hadjipapas and Georgios D. Mitsis

McGill University, Department of Bioengineering,
817 Sherbrooke St. W., Macdonald Engineering Building, Room 270
Montreal QC H3A 0C3

*: equal contribution

Correspondence and proofs to: Dr. Georgios D. Mitsis, Tel: +1-514-398-4344,

e-mail: georgios.mitsis@mcgill.ca

Keywords:

Potential financial interests: None

Abstract

The task of automated epileptic seizure detection and prediction, by using non-invasive measurements such as scalp EEG signals or invasive, intracranial recordings, has been at the heart of epilepsy studies for at least three decades. By far, the most common approach for tackling this problem is to examine short-length recordings around the occurrence of a seizure - normally ranging between several seconds and up to a few minutes before and after the epileptic event - and identify any significant changes that occur before or during the event. An inherent assumption in these studies is the presence of a relatively constant EEG activity in the interictal period, which is presumably interrupted by the occurrence of a seizure. Here, we examine this assumption by using long-duration scalp EEG data (ranging between 21 and 94 hours) in patients with epilepsy, based on which we construct functional brain networks. Our results suggest that not only these networks vary over time, but they do so in a periodic fashion, exhibiting multiple periods ranging between around one and 24 hours. The effects of seizure onset on the functional brain network properties were found to be considerably smaller in magnitude compared to the changes due to the inherent periodic cycles of these networks. Importantly, the properties of the identified network periodic components (instantaneous phase, particularly that of short-term periodicities around 3 and 5 hrs) were found to be strongly correlated to seizure onset. These correlations were found to be largely absent between EEG signal periodicities and seizure onset, suggesting that higher specificity may be achieved by using network-based metrics. In turn, this suggests that to achieve more robust seizure detection and/or prediction, the evolution of the underlying longer term functional brain network periodic variations should be taken into account.

1 Introduction

The task of detecting or predicting epileptic seizures has received tremendous attention for more than 30 years. Automated detection and prediction algorithms based on electroencephalographic (EEG) measurements attempt to characterize the transition from the inter-ictal to the ictal state, by identifying EEG patterns that significantly deviate from the inter-ictal state. For this reason, knowledge of the baseline inter-ictal properties is vital. In addition to examining the EEG signal properties originating from one or a few channels of interest, the use of functional connectivity patterns (Geier et al. 2015b) has been also suggested as a promising approach, as it may capture the underlying mechanisms in more detail and consequently improve our understanding of the emergence of epileptogenesis and ictogenesis. Functional brain networks are often described using concepts from complex systems and network theory, aiming to quantify the interplay between the dynamic properties of network constituents (i.e., nodes and links) and the network topology (Geier et al. 2015b).

In the majority of brain network studies on epilepsy, global properties of epileptic networks around seizure onset have been characterized using measures such as clustering coefficient, shortest path length/ efficiency or synchronizability (Lehnertz et al. 2014). Additional recent studies have explored the relevance of local network properties – such as the importance of individual nodes (Koschützki et al. 2005; Rubinov and Sporns 2010) – in the context of seizure dynamics (Kramer et al. 2008; Wilke et al. 2011; Varotto et al. 2012; Burns et al. 2014; Zubler et al. 2014; Geier et al. 2015a). Findings achieved so far for these seizure networks are quite intriguing, given the similarity of their topological evolution across different types of epilepsies, seizures, medication, age, gender, and other clinical features, which might point to a common biophysical mechanism underlying ictogenesis. This similarity, however, is contrasted by strong intra- and inter individual fluctuations of local and global statistical network properties seen for the temporal evolution of epileptic brain networks over periods of days (Kuhnert et al. 2010; Kramer et al. 2011; Geier et al. 2013).

The influence of the circadian rhythm on EEG signal properties, which results approximately in a main 24-hour periodicity, has been demonstrated for almost half a century (Scheich 1969). Some studies related to EEG-based epilepsy detection and prediction have also demonstrated the effect of the circadian rhythm. For instance, Kreuz et

al. (2004) studied one patient suffering from epilepsy and observed that certain intracranial channel combinations reflect the circadian rhythm. Schad et al. (2008) observed, for a subset of their patient population, the effect of the circadian rhythm on features obtained from the spiking rate, i.e. the rate at which local slopes cross a specified threshold, of both scalp and intracranial EEG.

The relation of seizures to sleep stages has also been examined. Bazil and Walczak (1997) revealed that sleep affects secondary generalization of partial seizures, especially those originating in the temporal lobe, and also that frontal lobe seizures occur more often during sleep than temporal lobe seizures. Minecan et al. (2002) confirmed earlier studies showing that seizure rate was higher in non-REM sleep compared to REM sleep and demonstrated that on the descent from lighter into deeper levels of sleep, seizures are more likely to occur. Bruzzo et al. (2008) tested the efficacy of permutation entropy (PE) to detect dynamic complexity changes on scalp EEG data showed a sensitivity to changes in vigilance state. The changes of PE during the preictal phase and at seizure onset coincided with changes in vigilance state, restricting its possible use for seizure prediction on scalp EEG.

Schelter et al. (2006) investigated the distribution of false seizure predictions with regards to the circadian rhythm and their relation to the sleep-wake cycle, and revealed that the majority of false predictions in non-REM sleep are associated with sleep stage II. More recently, Schelter et al. (2011) presented a strategy to avoid false seizure predictions by taking into consideration the circadian rhythms and using adaptive thresholds. Navarro et al. (2005) showed that different vigilance states have an influence on EEG measures.

Periodicities in the functional brain networks of healthy subjects have been studied in (Ferri et al. 2007, 2008), where it was shown that these networks moved towards a small-world organization (high clustering coefficient and small characteristic path length) during the transition from wakefulness towards sleep. Furthermore, the same authors used a shorter time scale known as Cyclic Alternating Pattern (CAP) (Terzano et al. 1985, 1988), recurring at intervals up to 1 min long, and demonstrated that the small-world organization is slightly but significantly more evident during the CAP A1 subtypes. Regarding patients with epilepsy, the existence of periodic fluctuations in the properties of functional brain networks was investigated in (Kuhnert et al. 2010), who observed that these fluctuations are significantly more pronounced than the ones seen during seizure activity and status epilepticus. Specifically, for the majority of patients in their study, a strong peak was observed in the range of 20–30 h, and averaging the normalized power spectral density estimates from all patients revealed a strong component at about 24 h with less pronounced

contributions at the sub-harmonics at about 12 and 8 h. They suggested that a large fraction of the temporal variability of their global network characteristics can be attributed to processes acting on timescales of hours to days, possibly with strong contributions of daily rhythms. Geier et al. (2015b) investigated the long-term evolution of degree-degree correlations (assortativity) in functional brain networks from epilepsy patients. They observed large fluctuations in time-resolved degree-degree correlations ranging from assortative to dissortative mixing, exhibiting some periodic temporal structure which can be attributed, to a large extent, to daily rhythms. Lastly, they claimed that relevant aspects of the epileptic process, particularly possible pre-seizure alterations, contribute marginally to the observed long-term fluctuations. Lehnertz et al. (2014) also showed that the functional brain networks of patients with epilepsy exhibit long-term fluctuations and that the epileptic focus is not consistently the most important node in the network, but node importance drastically varies over time. On the other hand, Kramer et al. (2011) identified the pattern of connections that occur persistently across time in the functional brain networks of patients with epilepsy.

In addition to the circadian and sleep-related periodicities mentioned above, other types of EEG signal periodicities have also been revealed. Kaiser et al. (Kaiser and Sterman 1994; Kaiser 2008) studied healthy subjects for twelve hours during the daytime wakefulness and identified a weak ultradian modulation with a cycle of approximately 90-120 min in the 9-11 Hz frequency band, and a slower and stronger temporal modulation with 4 hours period in the 11-13 Hz band. Chapotot et al. (2000) discovered a strong 3-4-hour periodicity in the EEG power during daytime, which was most pronounced in the fronto-central frequencies over 22.5 Hz as well as in parietal alpha activity.

Thus, long-term periodicities (hours/days) in scalp EEG signals are existent and possibly bear a relation to the occurrence of seizures. However, most epilepsy-related studies only utilize short segments of data around seizures and attempt to detect short-term changes immediately preceding or following a seizure. A key notion that remains poorly understood is the definition of an appropriate inter-ictal baseline. Given the above evidence about the periodic variations of this baseline, epileptic seizures and their detection/prediction may depend on the state of these variations. This question can only be addressed in continuous, long-duration data of patients with epilepsy, which is what we aimed to do in this study, using scalp EEG data. Specifically, we construct functional brain networks and examine their structure over multiple time scales by using graph-theoretic measures in order to summarize network properties. The results reveal periodicities over

different time scales in these properties and suggest that these may affect reliable detection of the transition from the interictal to ictal state, as they were found to be strongly correlated to seizure onset using circular statistics. We also demonstrate periodicities in the topology of functional brain networks by using a novel measure based on the graph edit distance measure.

2. Methods

2.1 EEG recording and preprocessing

Long-term video-EEG recordings were collected from nine patients with epilepsy and one patient with psychogenic seizures in the Neurology Ward of the Cyprus Institute of Neurology and Genetics. Six patients were monitored using the XLTek scalp EEG recording system (Patients 1-6), while the remaining four were monitored with the Nicolet system (Patients 7-10). Table 1 summarizes the duration of the recordings, as well as the number and type of seizures of each patient. Seizures and sleep intervals were identified and marked by specialized neurophysiologists (coauthors ESP and SSP).

Table 1: EEG recordings

Patient	Length of Recordings	Number of Seizures	Type of Seizures
1	46h	1	Focal
2	22h	2	Focal
3	68h	2	Focal
4	94h	1	Generalized
5	36h	1	Generalized
6	24h	0	Psychogenic
7	21h	1	Focal
8	71h	2	Focal
9	27h	6	Generalized
10	69h	4	Focal

Twenty-one electrodes were placed according to the 10-20 international system with two additional anterotemporal electrodes. In addition, four electrodes were used to record the electrooculogram (EOG) and electrocardiogram (ECG) signals respectively. The data were recorded at a sampling rate of 200Hz and 500Hz for the XLTek and Nicolet systems respectively, using a cephalic reference that was not part of the scalp derivations used to display the recorded channels. The EEG and EOG signals were band-pass filtered between 1 and 45Hz

to remove line noise and muscle artifacts. Next, the Lagged Auto-Mutual Information Clustering (LAMIC) algorithm (Nicolaou and Nasuto 2007; Daly et al. 2013) was applied in order to remove ocular artifacts using simultaneously recorded EOG recordings (2 channels) as reference signals (Ziehe and Müller 1998; Nicolaou and Nasuto 2003).

Subsequently, the data was converted to the bipolar montage, as it has been suggested that this montage is more robust to volume conduction effects (Christodoulakis et al. 2015). In this montage, pairs of EEG electrodes placed in nearby locations of the scalp are used to obtain the time-series by subtracting the corresponding measurements, forming the pairs Fp1-F7, F7-T3, T3-T5, T5-O1, Fp2-F8, F8-T4, T4-T6, T6-O2, Fp1-F3, F3-C3, C3-P3, P3-O1, Fp2-F4, F4-C4, C4-P4, P4-O2, Fz-Cz and Cz-Pz.

2.2 Functional brain network construction

Having obtained the artifact-free bipolar time series after the preprocessing stage, we construct the functional brain networks in the following manner. Each bipolar time series, e.g. Fp1-F7, corresponds to a node on the network, representing the area on the scalp that lies between the two electrodes, i.e. the area between Fp1 and F7. Note that nodes do not change over time. We then identify edges (i.e. connections) between nodes by quantifying time- and frequency-domain correlations between the corresponding EEG time series. In order to track network related changes over time, we use 5-second non-overlapping windows. Specifically, for each window, we quantify the correlation between all-time series pairs, using one of the following measures: cross-correlation function, corrected cross correlation, and coherence (see subsections 2.2.1-2.2.3). We finally produce binary graphs by using a threshold that is specific to each correlation measure as discussed in Section 2.2.4. Figure 1 demonstrates a representative network.

Figure 1: Functional brain network constructed from bipolar scalp EEG signals

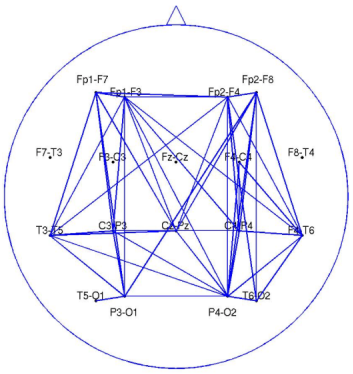

2.2.1 Cross-correlation

For any pair of time series, **x(t)** and **y(t)**, the normalized cross-correlation is calculated as follows:

$$\boldsymbol{C_{xy}(\tau) = \frac{1}{n-\tau}\sum_{t=1}^{n-\tau}\left(\frac{x(t)}{\sigma_x}\right)\left(\frac{y(t+\tau)}{\sigma_y}\right)} \qquad \textbf{(1)}$$

where σ_x and σ_y are the standard deviations of x and y respectively. $\boldsymbol{C_{xy}}$ is computed for a range of values for the lag τ, which depends on the sampling frequency; for the required range of [-100 100] msec chosen here, τ lies between [-20 20] and [-50 50] time lags for the data recorded with the XLTek (200Hz sampling frequency) and Nicolet (500Hz sampling frequency) systems respectively. C_{xy} takes values between -1 and 1, with 1 indicating the perfect linear positive correlation, -1 perfect linear negative correlation and 0 no correlation. The maximum of the absolute value of cross-correlation, $\boldsymbol{max_\tau|C_{xy}|}$, over the chosen range of τ values, is used to quantify the degree of correlation between the two signals within a given window.

2.2.2 Corrected cross-correlation

Cross-correlation often takes its maximum at zero lag in the case of scalp EEG measurements. Consistent zero-lag correlations could be due to volume conduction effects, whereby currents from underlying sources are conducted instantaneously through the head volume to the EEG sensors (i.e., assuming that scalp potentials have no delays compared to their underlying sources (quasi-static approximation) (Christodoulakis et al. 2015). In principle, true direct interactions between any two physiological sources will typically incur a nonzero delay due to transmission speed, provided that the sampling frequency is high enough

to capture such delays. In order to measure true interactions not occurring at zero lag, we calculate the corrected cross-correlation, which is a measure of the time-series' asymmetry, as defined in (Nevado et al. 2012), by subtracting the negative-lag part of $\mathbf{C_{xy}(\tau)}$ from its positive-lag counterpart:

$$\overline{\boldsymbol{C}}_{\boldsymbol{xy}}(\boldsymbol{\tau}) = \boldsymbol{C}_{\boldsymbol{xy}}(\boldsymbol{\tau}) - \boldsymbol{C}_{\boldsymbol{xy}}(-\boldsymbol{\tau}) \qquad \text{for } \tau > 0 \qquad \textbf{(2)}$$

Note that $\overline{\boldsymbol{C}}_{\boldsymbol{xy}}(\boldsymbol{\tau})$ provides a lower bound estimate of the nonzero-lag cross-correlations and is notably smaller than $\boldsymbol{C}_{\boldsymbol{xy}}$. As in the case of cross-correlation, the maximum in the range of desired time lags is taken as the degree of correlation.

2.2.3 Coherence

Coherency may be viewed as the equivalent measure of cross-correlation in the frequency domain; it measures the linear correlation between two signals *x* and *y* as a function of the frequency *f*. It is defined as the cross-spectral density, $S_{xy}(f)$, between *x* and *y* normalized by the auto-spectral densities, $S_{xx}(f)$ and $S_{yy}(f)$, of *x* and *y* respectively. Coherency is a complex number, as the cross-spectral density is complex, whereas the auto-spectral density function is real. Therefore, in many cases coherence (or the squared coherence), which is defined as the magnitude of coherency (or its square), is employed as a measure of correlation in the frequency domain, i.e.:

$$\boldsymbol{k}_{\boldsymbol{xy}}(\boldsymbol{f}) = \frac{|\langle \boldsymbol{S}_{\boldsymbol{xy}}(\boldsymbol{f})\rangle|}{\sqrt{|\langle \boldsymbol{S}_{\boldsymbol{xx}}(\boldsymbol{f})\rangle||\langle \boldsymbol{S}_{\boldsymbol{yy}}(\boldsymbol{f})\rangle|}} \qquad \textbf{(3)}$$

The value of $k_{xy}(f)$ ranges between 0 and 1, with 1 indicating perfect linear correlation and 0 no correlation between *x* and *y* at frequency *f*. We calculated the maximum coherence value for the broadband EEG signals (1-45Hz), as well as for each EEG frequency band; delta (1-4Hz), theta (4-8Hz), alpha (8-13Hz), beta (13-30Hz) and gamma (30-45Hz), in order to assess the degree of correlation between the two signals within these bands separately. The maximum coherence value within each frequency band is used to quantify correlation.

2.2.4 Network binarization

In order to obtain a binary (rather than weighted) network, i.e. a network where connections exist only between strongly correlated nodes, a threshold is set, the value of which depends on the employed correlation measure. Edges with weight values larger than the specified threshold are included in the graph (with a weight of 1), while edges with values less than the threshold are removed (weight is set to 0). Therefore, weight annotations are no longer necessary on the edges. For the three correlation measures that have been used in this study (as well as alternative ones), e.g. see (Christodoulakis et al. 2015), we experimented with various threshold values. In all cases, it was found that different threshold values yield very similar results in terms of the observed periodicity patterns, provided that the threshold value is not too high (e.g. close to one for correlation or coherence) yielding disconnected graphs, or too low (close to zero), yielding densely/fully connected graphs. For threshold values between these two extremes, the graphs exhibited similar properties, as shown in (Christodoulakis et al. 2015) for shorter data segments, and in supplementary material (Figure A.1) for a representative long-duration data set (94 hours for Patient 4). From Figure A.1 it is evident that the observed patterns and periodicities of the network properties (average degree in this figure) are similar for threshold values between 0.2 and 0.8. The chosen threshold value determines the actual value of the network properties, but does not considerably affect our results otherwise (we are interested in the variation of these properties over time and not their absolute value). Hence, we have chosen the threshold independently for each correlation measure, aiming to have similar average degree values for all measures. Specifically, for cross-correlation and coherence, the threshold was set to 0.65, while for corrected cross-correlation it was set to 0.20. We also used surrogate data to construct binary networks; however, they were found to yield rather densely connected networks and the results were similar to those obtained by simply setting a fixed, low threshold value. Hence, we have chosen the former, simpler thresholding method.

2.3 Functional brain network evolution

For each subject, the evolution of the functional brain networks over time was quantified in two ways. First, we quantified how different properties of the graph changed over time, namely average degree, global efficiency and clustering coefficient (subsections 2.3.1-2.3.3). Furthermore, we also performed direct comparisons of the network topologies at different times by means of the graph edit distance, which quantifies the dissimilarity between

different graphs (Section 2.3.4). In the following, let n denote the number of nodes of the network (in our case n=18) and N the set of all nodes.

2.3.1 Average degree

The degree k_i of a node i is defined as the number of nodes j in the network to which node i is connected to via an edge, e_{ij}; that is, the number of edges incident to i. The average network degree is given by:

$$\boldsymbol{K = \frac{1}{n} \sum_{i \epsilon N} k_i} \qquad \textbf{(4)}$$

The average degree of a graph quantifies how well connected the graph is.

2.3.2 Global efficiency

Although the average degree reflects the average number of connections any network node may have, it does not provide any information regarding the actual distribution of the edges and, hence, how easy it is for the information to flow in the network. This can be captured by the shortest (or geodesic) path length d_{ij} between a pair of nodes i and j. It is defined as the minimum number of edges that have to be traversed to get from node i to j. The characteristic path length is defined as the average shortest path length over all pairs of nodes in the network:

$$\boldsymbol{L = \frac{1}{n(n-1)} \sum_{i,j \epsilon N, i \neq j} d_{ij}} \qquad \textbf{(5)}$$

However, the characteristic path length is well defined only for pairs of nodes that are connected through a path. If any pair of nodes i and j is not connected through a path, the shortest path length between i and j is $d_{ij} = \infty$, hence the average shortest path length for the network becomes $L = \infty$. A workaround for this is to consider only pairs of nodes that are connected through a path, but this does not reflect the connectivity of the entire network. To overcome this, Latora and Marchiori (2001) defined the efficiency between a pair of nodes as the inverse of the shortest distance between the nodes, $\boldsymbol{1/d_{ij}}$. Global efficiency is defined as the average efficiency over all pairs of nodes (Latora and Marchiori 2001):

$$\boldsymbol{E = \frac{1}{n(n-1)} \sum_{i,j \epsilon N, i \neq j} \frac{1}{d_{ij}}} \qquad \textbf{(6)}$$

Note that in this case, when a path between two nodes does not exist, the efficiency of the path is zero.

2.3.3 Clustering coefficient

A cluster in a graph is a group of nodes that are highly interconnected. The clustering coefficient (Watts and Strogatz 1998) *Ci* of a node *i* is defined as the fraction of existing edges between nodes adjacent to node *i* over the maximum possible number of edges:

$$C_i = \frac{2t_i}{k_i\,(k_i - 1)} \qquad (7)$$

where k_i is the degree of node *i*, and t_i denotes the number of edges $e_{jj'}$ between pairs of nodes *j* and *j′* that are both connected to *i*. The clustering coefficient, *C*, of the network is the mean clustering coefficient across all nodes.

$$C = \frac{1}{n}\sum_{i \in N} C_i \qquad (8)$$

2.3.4 Graph edit distance

Using the graph properties defined above, the general characteristics of two (or more) functional brain networks corresponding to different times may be compared. If the value of a network property (e.g. degree, clustering coefficient, efficiency) corresponding to one network differs substantially from the value of the same property corresponding to some other network, it is reasonable to assume that these two networks differ in their topology as well. However, comparing networks with similar network property values can be inconclusive. Consider, for instance, two networks with average degree 5. It is impossible to conclude whether these two networks are similar in structure by the average degree alone; for example, one of the networks could have its edges equally distributed among the nodes (each node having degree 5), while the other could have a large number of low degree nodes and a few hubs possessing a large number of connections. In order to more accurately quantify topological difference between graphs, we compare, additionally, every pair of graphs directly in terms of their structure, using the graph edit distance measure. The graph edit distance (Dickinson et al. 2003) estimates graph similarity in terms of the minimum number of insertions and deletions of either nodes or edges

that must take place in one graph in order to make it identical to the second. When the two graphs share the same set of nodes, as is the case for EEG functional brain networks, the distance between the graphs is defined as the minimum number of edge insertions and deletions that are necessary in order to make the two graphs identical. Essentially, the graph edit distance g_{AB} between two functional brain networks A and B is equal to the number of edges that exist only in one of the two graphs. Note that graph edit distance is a symmetric measure, since an insertion of an edge in one graph is equivalent to a deletion in the other.

2.3.4 Periodicity estimation

One of the main goals of the present work was to characterize the periodicities that arise in functional brain network characteristics over time. We achieve this by: first, monitoring properties that summarize key aspects of the networks, and second, examining the actual structure of the networks using the graph edit distance. Each of the three summative network properties -average degree, global efficiency, and clustering coefficient - provides a single value per network, thus forming a time series across time. A simple method for identifying periodicities in these time series, is by computing their normalized autocorrelation function and then finding the average distance between consecutive peaks. This method is adequate for showing the strongest periods - such as the circadian rhythm - however, it is not accurate enough for showing smaller periodicities in the time series. To this end, we utilized the Lomb-Scargle periodogram to obtain the power spectral density (PSD) of each network property and more details are summarized in A.2. The periodogram, apart from being calculated for the full-length network property time series, was also calculated separately for sections corresponding to sleep and wake times.

As mentioned earlier, similarity between network properties does not necessarily imply similarity in network structure; consequently, periodicity in network properties does not necessarily imply structure/topology periodicity. For this reason, we investigated the existence of periodicities in the network structure by developing a novel measure based on the graph edit distance. Specifically, we consider the course of the functional brain network over time as a vector, $\mathbf{A}$, of graphs, whereby $\mathbf{A}(t)$ corresponds to the functional brain network at time lag t (and each time lag corresponds to one 5-sec window). We then compare this vector with shifted copies of itself and for each shift value τ, we calculate the average graph edit distance (ged, in short) between all network pairs that are separated by τ time lags:

$$G_{ged}(\tau) = \frac{1}{n-\tau}\sum_{t=1}^{n-\tau} g_{A(t)A(t+\tau)} \qquad (9)$$

Inspired by the autocorrelation function, this is a novel measure for directly detecting periodic changes in the network structure over time, as opposed to the indirect method of monitoring network summative properties. Note that, for any shift value τ, the lower the average graph edit distance value $G_{ged}(\tau)$ is, the more similar the corresponding graphs are.

2.3.5 Circular Statistics

To investigate the relation of seizure onset to network periodicities, we calculated the instantaneous phase at seizure onsets for each periodic component and obtained a phase distribution for each of these components. Subsequently, we used circular statistics to examine whether seizure onsets occurred at specific/preferred phases (as opposed to random phases). To this end, we first performed zero-phase digital filtering of the average degree time series to obtain band limited signals around the main identified periodicities (±0.5hr before and after the main period of each component). Specifically, we investigated the following periodic components: 3.6, 5.4, 12 and 24hrs, as they were found to be pronounced for all patients (Table 3). Subsequently, we applied the Hilbert transform on the band limited signals to calculate the instantaneous phase of each periodic component at the time of seizure onset for all patients (Klingspor 2015).

Circular statistics are suitable for data that are defined within an angular scale, as in the present case, whereby there is no designated zero and, in contrast to a linear scale, the designation of high and low values is arbitrary (Berens 2009). In this context, the mean resultant vector after transforming the data points to unit vectors in the two-dimensional angular plane is given by:

$$\bar{\boldsymbol{r}} = \frac{1}{N}\sum_{I} \boldsymbol{r_i} \qquad (10)$$

where $\mathbf{r_i}$ is the unit vector. The length of the mean resultant vector is a crucial quantity for the measurement of circular spread or hypothesis testing in directional statistics. The closer it is to one, the more concentrated the data sample is around the mean direction. The resultant vector length is computed by:

$$R = \|\bar{\boldsymbol{r}}\| \qquad (11)$$

The circular variance, which is closely related to the length of the mean resultant vector (Berens 2009), is defined as:

$$S = 1 - R \qquad \textbf{(12)}$$

In contrast to the variance on a linear scale, the circular variance *S* is bounded within the interval [0, 1]. It is indicative of the spread in a data set. If all samples point into the same direction, the corresponding mean vector will have length close to 1 and the circular variance will be small. If the samples are spread out evenly around the circle, the mean vector will have length close to 0 and the circular variance will be close to its maximum value of one. We investigated whether phase values at seizure onset times were distributed uniformly around the circle from 0 to 2π or whether a common mean direction existed by using the instantaneous phase obtained for all seizures and patients. We applied the Rayleigh test to assess significance with the following common null hypothesis H_0: the population is distributed uniformly around the circle, with alternative hypothesis H_1: the population is not distributed uniformly around the circle. The Rayleigh test computes the resultant vector length *R* that suggests a non-uniform distribution (Fisher 1993). It is particularly suited for detecting a unimodal deviation from uniformity. The approximate *p*-value under H_0 is computed as (Zar 1999):

$$P = e^{\left(1+4N+4\left(N^2R_n^2\right)(1+2N)\right)} \qquad \textbf{(13)}$$

where $R_n = R \times N$. A small *p* value (<0.05) indicates a significant departure from uniformity and indicates rejection of the null hypothesis. This was done for all seizures (twenty in total) corresponding to nine different patients.

To account for the fact that we had multiple seizures for some subjects, we also created groups of nine samples (one seizure per patient) for all possible combinations and investigated periods (3.6h, 5.4h,12h and 24h) in order to perform correction for multiple comparisons (Zar 1999). Note that for the 24 hr periodic (circadian) component, these groups included six samples only, since the recordings of six patients were longer than 24 hours. Subsequently, we applied the Rayleigh test (Zar 1999) to compute the corresponding corrected *p*-values. All the above quantities were computed with CircStat, which is a Matlab (Math works, Natick MA) toolbox related to circular statistics.

3 Results

With the exception of Subsection 3.6, the results presented below correspond to Patient 4, since for this patient the longest recording was obtained (94 hours). Similar results were obtained from all ten patients, as discussed in Subsection 3.6.

3.1 Periodicities in network properties

3.1.1 Time domain

Cross-correlation and corrected cross-correlation were used for assessing pairwise correlations and constructing the corresponding functional brain networks (Section 2.2). Figure 2 (a-c) shows the time course of the three network properties of interest (average degree, global efficiency and clustering coefficient). It is evident that functional brain networks are less connected and less clustered during the time when the patient is awake compared to sleep (grey shaded bars). This pattern occurs periodically, in cycles of approximately 24 hours, a fact that is further illustrated by the autocorrelation sequence (Figure 2 (e-f)) of the three network properties, which also demonstrate a clear periodic pattern with a main period equal to around 24 hours. Very similar results were obtained when the corrected cross-correlation was used for constructing the networks (Figure 3), with a main 24-hour period evident. Along with the 24-hour cycles, it can be observed that additional periodic components at smaller time scales co-exist in the time course of the obtained functional brain networks; note, for example, the spikes that occur at both awake- and sleep-times separated on average by approximately 75 minutes. These weaker periodicities, are examined in detail in Subsection 3.2.

Figure 2: Top row: Average degree (a), global efficiency (b), and clustering coefficient (c), of the functional brain networks of Patient 4 as a function of time, using cross correlation for assessing pairwise correlations. For presentation purposes, the obtained network properties have been smoothed by removing the mean from the signal. The vertical dashed line indicates seizure onset and the grey bars indicate sleep intervals. Bottom row: The autocorrelation sequences of the three network properties ((d)-(f)). We can clearly observe a periodic pattern with a main period equal to around 24 hours.

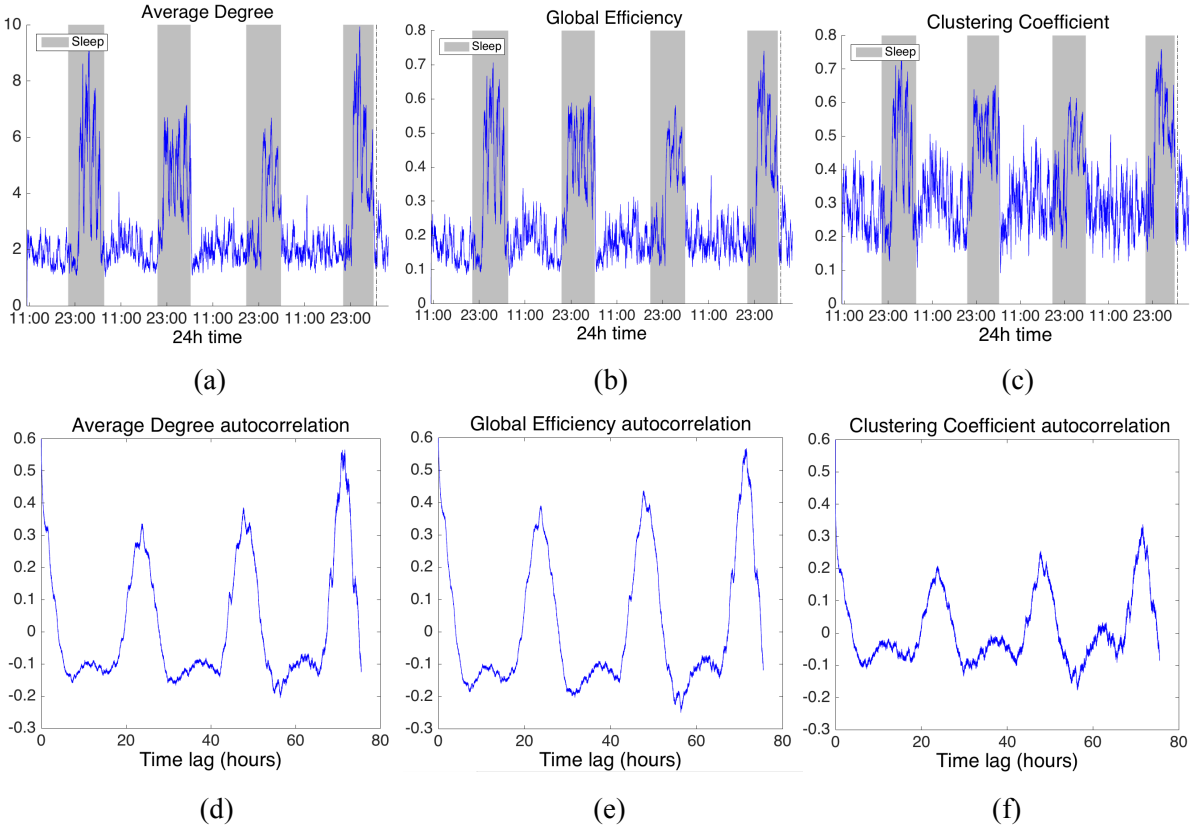

Figure 3: Average degree (a), global efficiency (b), and clustering coefficient (c), and their corresponding autocorrelation sequences (d)-(f), of the functional brain network of Patient 4 as a function of time using corrected cross-correlation for assessing pairwise correlations. We can clearly observe a periodic pattern with a main period equal to around 24 hours.

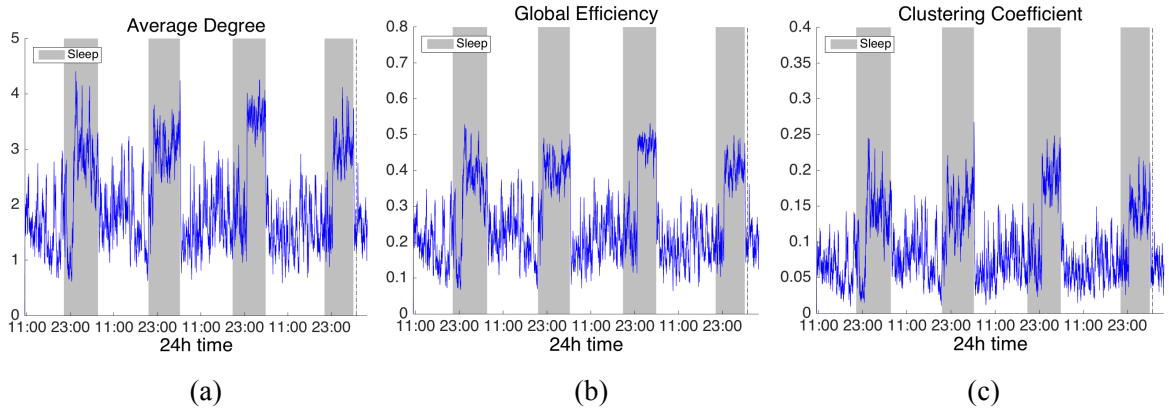

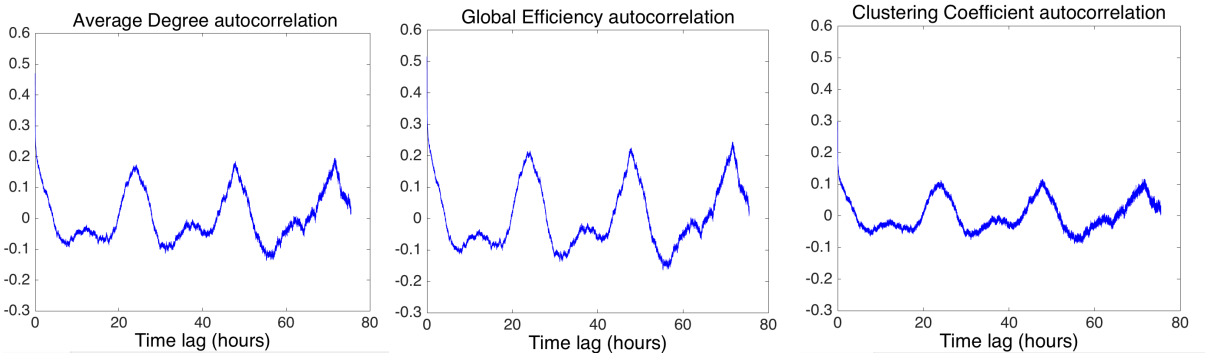

(d) (e) (f)

3.1.2 Frequency domain

In order to investigate brain network properties in different frequency bands, we constructed these networks using coherence as the correlation measure, whereby the maximum coherence value within each frequency band was used to quantify correlation. In the supplementary material, we present the average degree of the brain networks within the six frequency bands of interest (Figure A.2). Global efficiency and clustering coefficient are not shown separately, but they yielded similar periodicities within all bands. With the exception of the gamma band, the 24-hour periodicity is clear for all other frequency bands. In particular, the 24h period is more pronounced in the alpha band, followed by the beta band, and finally the delta and theta bands. The autocorrelation of the average degree in the broadband signal is similar to that in the alpha and beta bands, suggesting that these bands dominate the long-term broadband network properties.

3.2 Periodicities at smaller time scales

Apart from the obvious 24h periodicity in all network properties, periodicities at smaller time scales can also be observed (Figures 2-3, A.2). In this section, we investigate these periodicities in more detail. Figure 4 presents the periodogram of the average degree of the functional brain networks of Patient 4 constructed using the cross-correlation (Figure 2). The peaks in the periodogram correspond to periods and have been marked accordingly. We also present in the supplementary material the periodogram for the distinct sleep and awake intervals of the average degree for Patient 4 using cross-correlation (Figure A.3). The main peaks are summarized in Table A.1 in the supplementary material, whereby we consider a period found in one interval to be equal to that of another if they differ by half an hour at most. Table 2 summarizes all periods that have been identified for each of the patients we examined.

Note that the 24h periodicity is of course absent for patients whose recordings span less than 24h. We observed that for all patients the most pronounced periods were 3hr, 5hr, 12hr and 24hr. With regards to the difference between the networks at awake and sleep time, we observed that, except for Patient 7 all other patients demonstrated a similar trend, whereby all three network properties we examined increase during sleep-time. In the supplementary material, we present for all patients the 99% confidence interval of the difference between the average degree at sleep time minus the average degree at awake time (Figure A.4).

Figure 4: Periodogram of the average degree of the functional brain network of Patient 4 using cross-correlation. Top panel: entire periodogram of the signal, bottom panel: zoomed-in version (1-10 hours). We identified and marked periods that were common for all patients such as the 12 and 24hr period, and smaller periodicities such as 3 and 5hr.

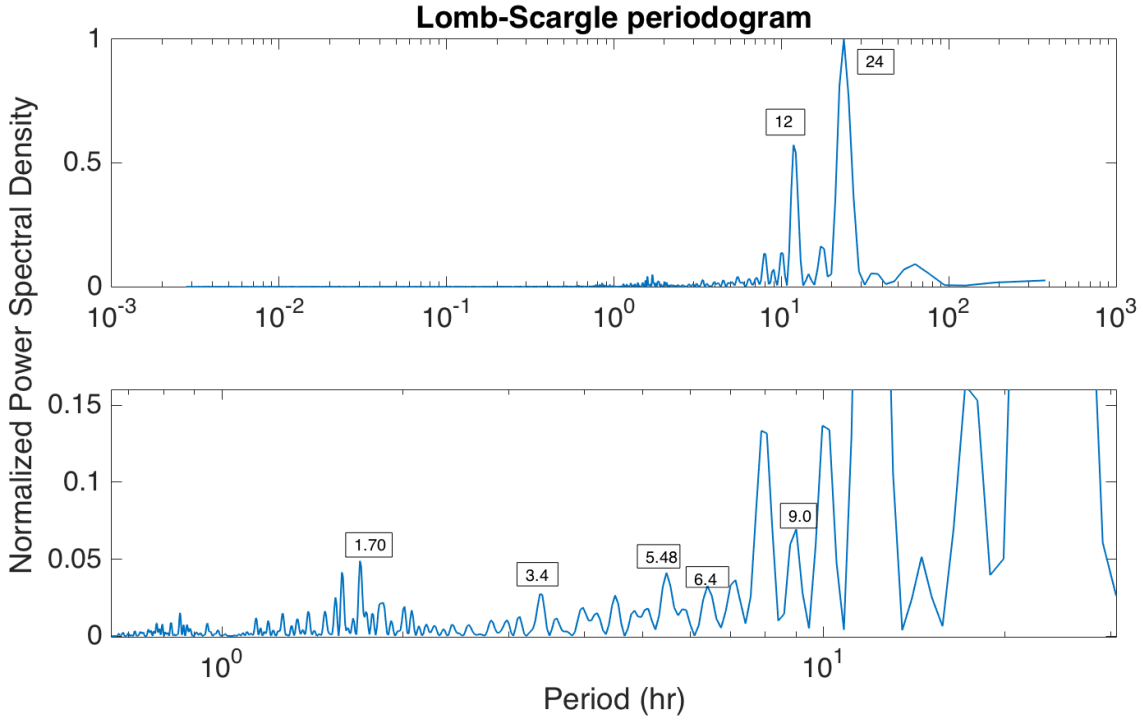

Table 2: All periods identified in the periodogram of the average degree for Patients 1-10.

Period	P1	P2	P3	P4	P5	P6	P7	P8	P9	P10
24.0	√	N/A	√	√	√	N/A	√	√	N/A	√
12.0	√	√	√	√		√		√	√	√
8.0	√		√	√	√			√		√
5.4	√	√	√	√	√	√	√	√	√	√
3.6	√	√	√	√	√	√	√	√	√	√
1.7	√	√		√		√		√	√	

3.3 Periodicities in network topology

In addition to examining the evolution of properties of functional brain networks over time, we also investigated evaluated the evolution of their topology using the novel procedure based on the graph edit distance (Section 2.4). Figure 5 shows the results for Patient 4, while results for all patients are presented in the supplementary material (Figure A.5). In this case, note that similarity is now indicated by local minima. The 24h period is again clearly visible. We further analyzed the average graph edit distance (Eq. 9) using the periodogram and we identified main periodic components at 12 and 24hrs (Figure 5), i.e. very similar to those calculated by the network properties for Patient 4. In a similar fashion, the periods identified for the remaining nine patients were similar to those identified by their summative network properties, suggesting that network topology is characterized by the same periodic components.

Figure 5: The periodicity in the network structure as calculated with the graph edit distance measure of graph comparison, as a function of the time lag for Patient 4. Up right is the PSD of the graph edit distance indicating the important periods at 12 and 24hr.

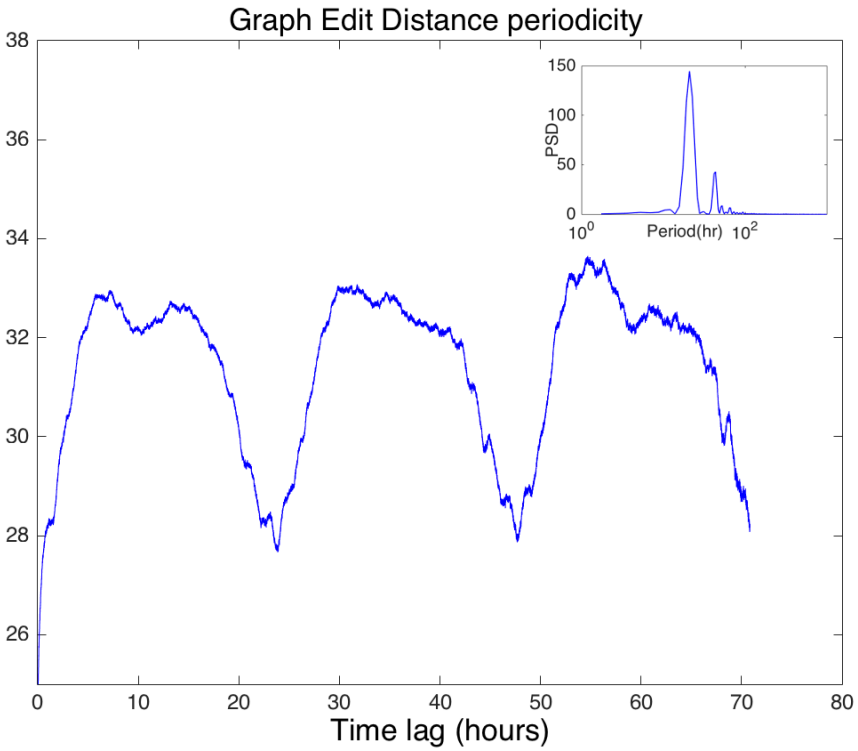

3.4 Periodicities in signal power

Having identified all these different, concurrent periods in the evolution of the functional brain networks over time, it is natural to question whether these periodicities are mainly due to the corresponding periodicities in the original EEG signals. To test this hypothesis, we calculated the power of the EEG channels within six frequency bands (broadband, delta, theta, alpha, beta and gamma) and show their long-term evolution in Figure 6. The results for all 10 patients have been very similar, with small variations as expected, depends on the length of the recordings. The influence of the circadian rhythm is evident, especially in the broadband, beta and gamma bands (note the difference to network properties, which did not exhibit periodicities in the gamma but rather in the alpha band). Also, there is a clear decrease in the EEG signal power during sleep time, as opposed to the increase in connectivity observed from the functional brain networks (Figures 2-3).

3.5 The effect of seizure

Figure 7 shows the Average Degree of Patient 4 at various scales around the seizure which occurs at approximately 91 hours after the beginning of the recording, when the network has been constructed using cross-correlation (see Figure 2(a)). In both plots (a) and (b) in Figure 7, whereby ±2 and ±5 minutes around the seizure onset are examined, an increase of connectivity slightly before seizure onset is apparent, which gradually decreases after the onset until it reaches levels lower than the pre-seizure connectivity some minutes later.

On the contrary, plots (c)-(f), on which segments of the Average Degree of length at least ±15 minutes long are presented, reveal a different picture: the changes in connectivity that one could attribute to the occurrence of the seizure when examining plots (a)-(b) are actually very small with regards to the recurring variations in the connectivity of the network that occur as part of the various cycles of the human brain.

In the previous subsections and here, we used Patient 4 - for whom we acquired the lengthiest scalp EEG recording, 94 hours - to showcase our results. However, for all 10 patients in our studies the results have been very similar, with small variations as expected.

Figure 6: Average signal power (blue) and standard deviation (grey) of all bipolar signals of Patient 4, at different frequency bands (broadband, delta, theta, alpha, beta and gamma). We can observe a periodic pattern around 24hr in all bands with similar results for all patients.

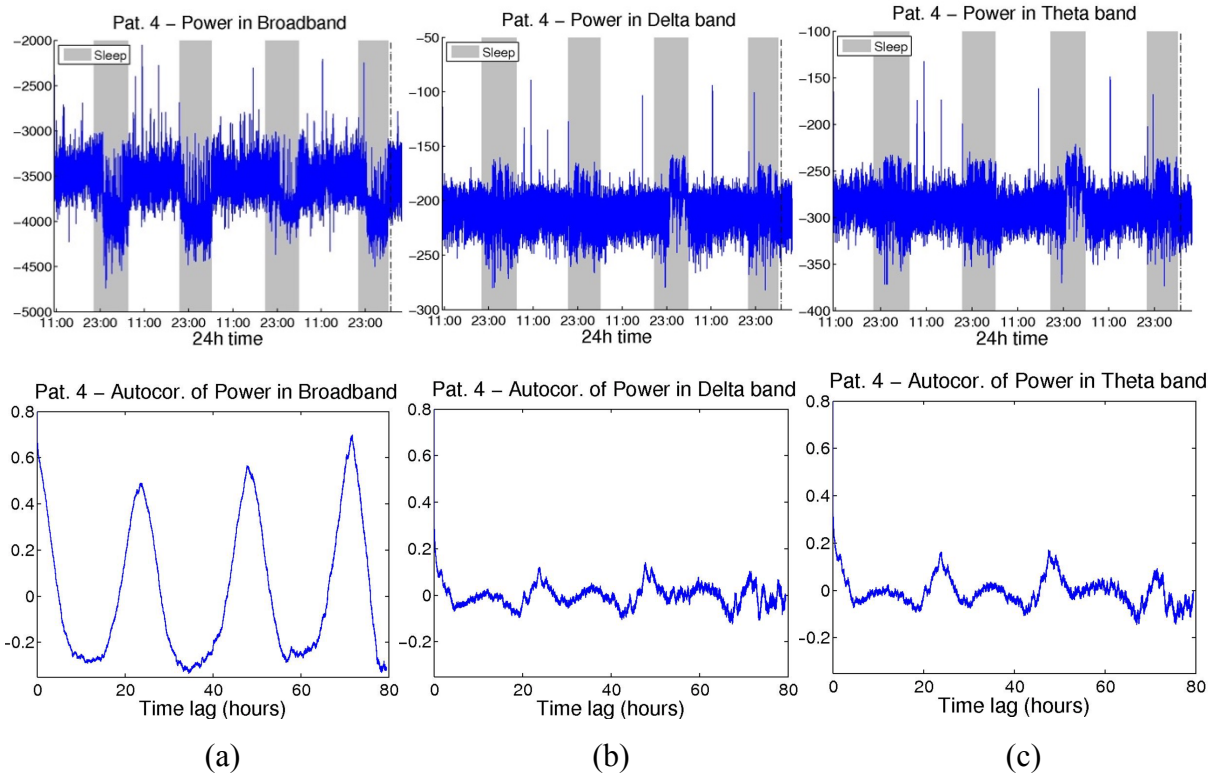

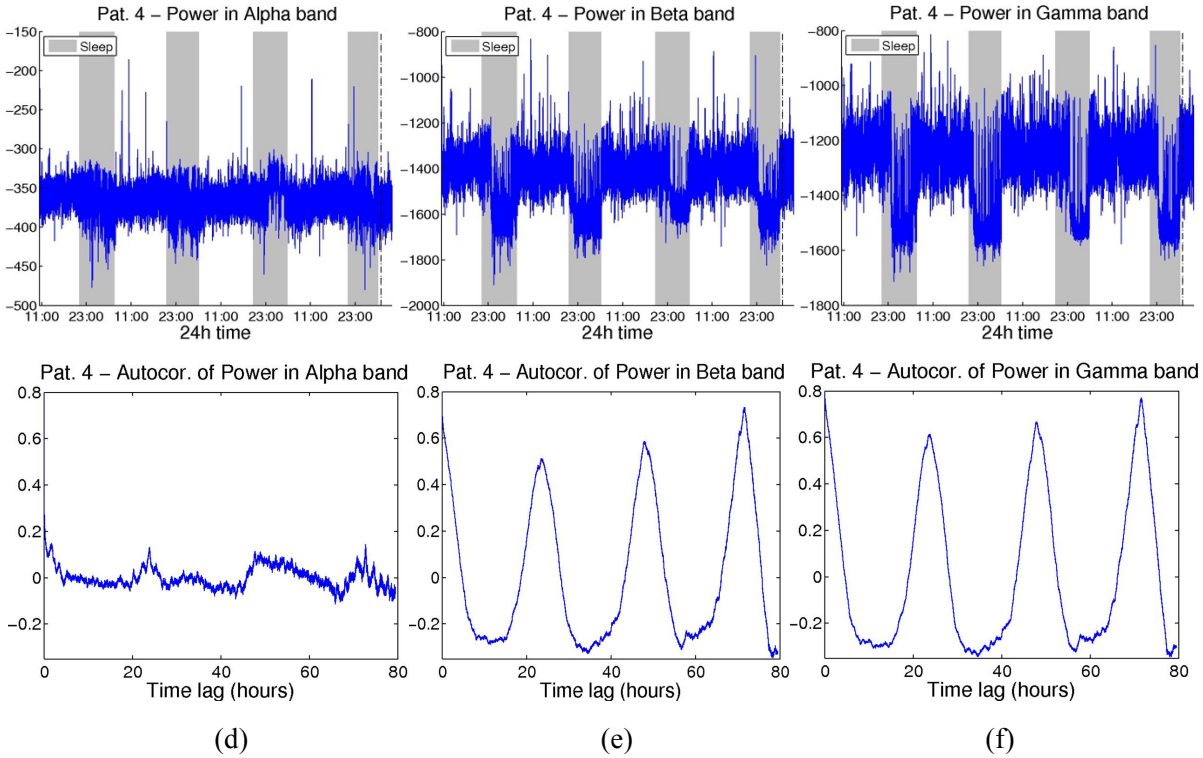

Figure 7: Average Degree (smoothed) around the seizure of the functional brain network of Patient 4 using cross correlation, at different scales: (a) ±2 minutes around seizure onset, (b) ±5 min, (c) ±15 min, (d) ±30 min, (e) ±1 hour, (f) ±2 hours. Seizure onset is indicated by the dashed vertical line, while the seizure end by the dotted line. There is an increase on average degree at the time of seizure which can be assume as local maxima (a-c) but in 24hr scale (d-f) the same variation are very small.

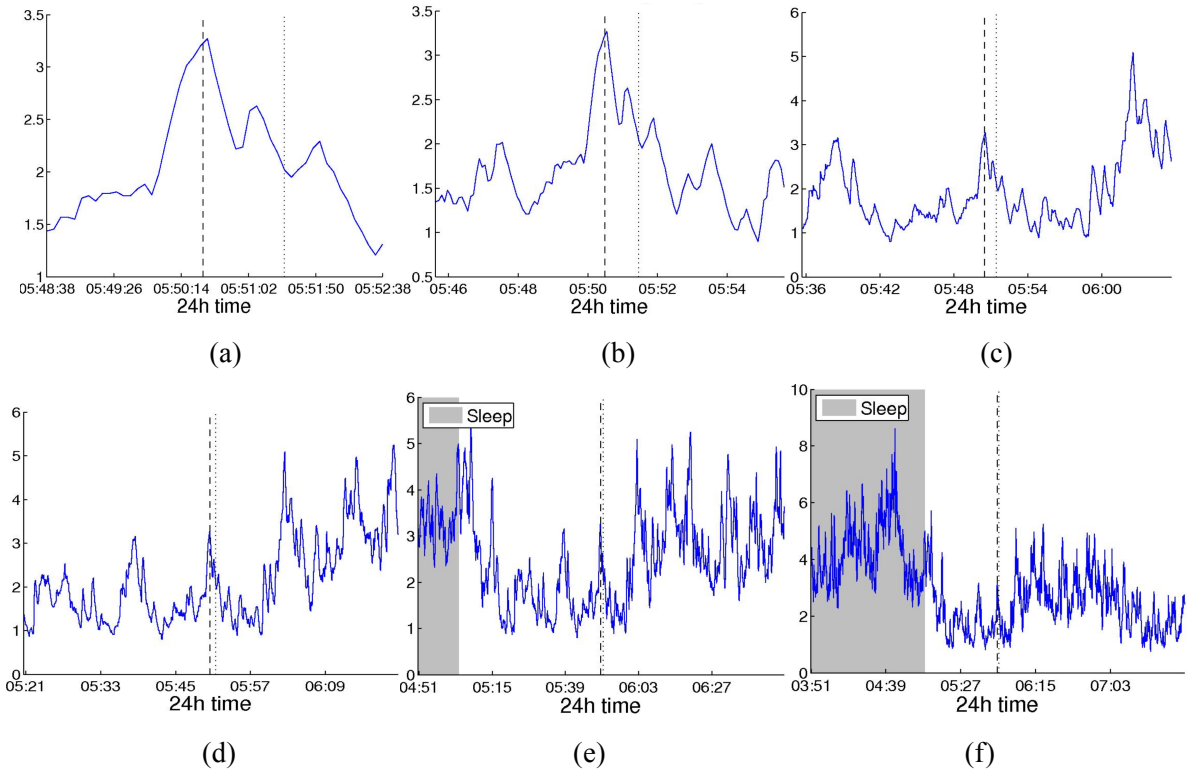

3.6 Circular Statistics

The instantaneous phases of the main identified periodicities (3.6h, 5.4h, 12h and 24h) are shown in Figure 8 for all seizures from nine patients. Note that during the recordings of Patient 6 no seizures were recorded and for this reason it has not been included in this analysis. The left panels show the instantaneous phases on the unit circle. The right panels show the corresponding angular histograms. The red and black lines indicate the direction and magnitude of the mean resultant vector. The green points indicate the instantaneous phases obtained through power of a bipolar channel of interest and the blue points the instantaneous phases obtained through degree.

The length of the mean resultant vector is a crucial quantity for the measurement of circular spread or hypothesis testing in directional statistics. Note that the closer it is to one, the more concentrated the data sample is around the mean direction. Table 3 represents the mean resultant vector, R and the circular variance, S of the phases obtained through degree and signal power. It is evident from all plots that instantaneous phases are not distributed uniformly, but seizures occur within specific phase ranges. Interestingly, this is more evident for the shorter (3.6h, 5.4h) periodicities compared to the longer ones. In contrast, the instantaneous phases obtained through power are uniformly distributed around the circle. The p-values of the Rayleigh's test are presented at Table 4.

To account for the fact that we had multiple seizures for some subjects, we performed multiple comparisons. To do so, we created multiple groups of nine samples (number of patients) each for all investigated periods 3.6h, 5.4h and 12h. For the circadian rhythm, the groups include six samples since not all patients have enough recordings. Each sample of the groups represents one seizure per patient. Thus, we test for difference between all groups for each periodicity separately. This is further corroborated by Table 4 which shows the corresponding p-values of Rayleigh's test for all groups for each instantaneous phase. The results indicate that the null hypothesis is rejected and that all groups of each instantaneous phase does not distributed uniformly around the circle.

Figure 8: Instantaneous phases at seizure onset for the: (a) 3.6h, (b) 5.4h (c) 12h and (d) 24h periodicities of all patients. The left panels present the unit circle and the phases as points for all seizures from all patients. The right panels present the angular histogram of the distribution. The blue points and the red line (R) represents the instantaneous phases obtained through degree for all patients. The green points and black line (R) represents the instantaneous phases obtained through the power for patients with generalized epilepsy and the magenta points and grey line (R) represents the instantaneous phases obtained through the power for patients with focal epilepsy.

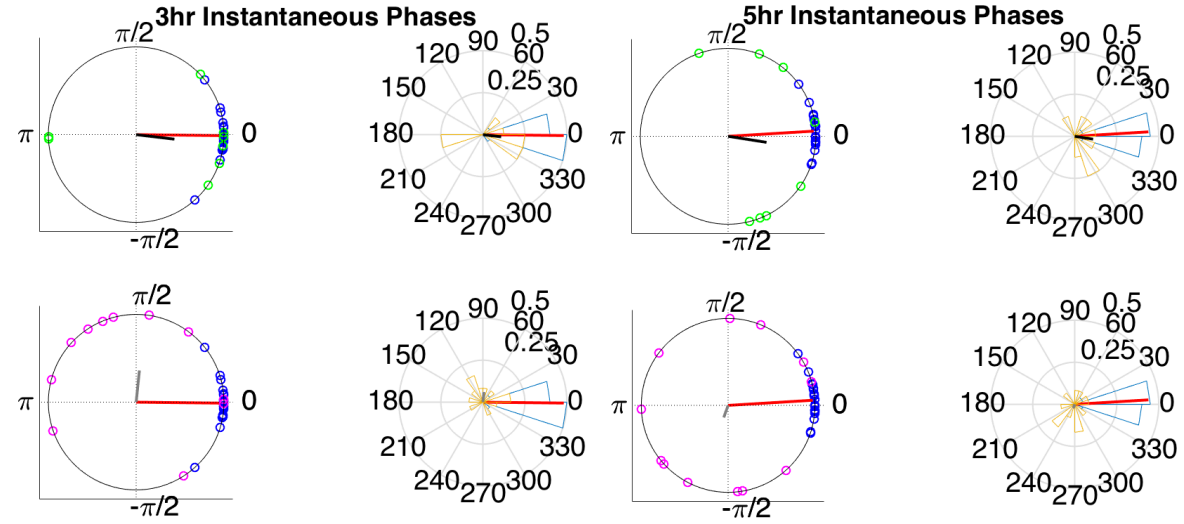

(a) (b)

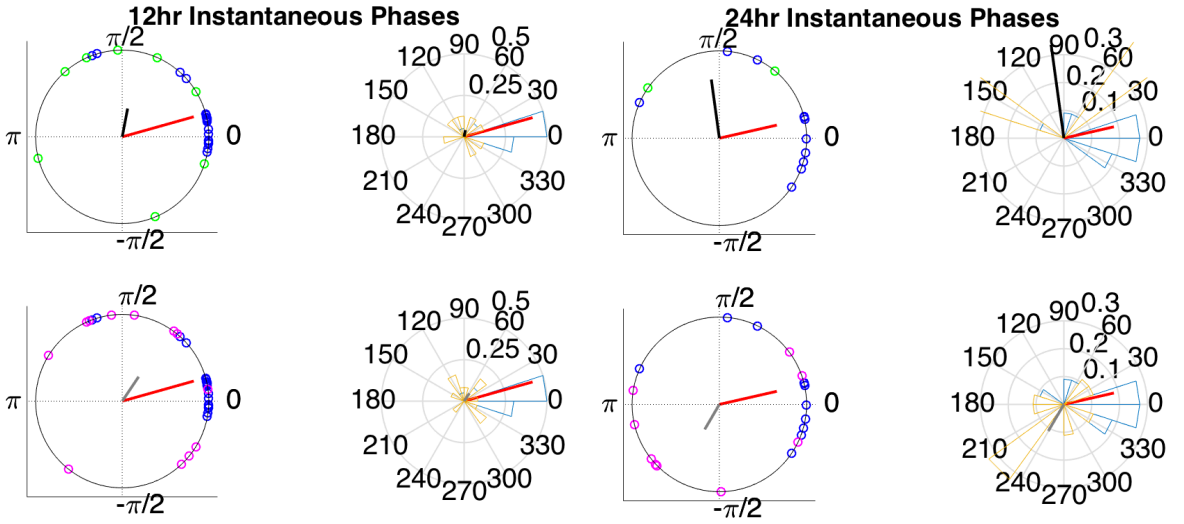

(c) (d)

Table 3: The values for the mean resultant vector, R and the circular variance, S of the phases obtained through degree and signal power.

	R	S	R	S	R	S	R	S
Signal	**3.6h**		**5.4h**		**12h**		**24h**	
Average Degree	0.97	0.02	0.98	0.02	0.85	0.14	0.72	0.28
Power	0.28	0.72	0.18	0.82	0.33	0.67	0.19	0.81

Table 4: P-values (uniform distribution of instantaneous phases) for the main periodic components: 3.6h, 5.4h, 12h and 24h.

Rayleigh's Test	**3.6h**	**5.4h**	**12h**	**24h**
Average Degree	1.4e-8	1.5e-8	2e-7	1.2e-6
Signal Power	0.22	0.52	0.11	0.68
Groups (Degree, max-value)	2.5e-5	2.4e-5	4.3e-4	0.02

4 Discussion

Seizure detection and prediction has proven over the years to be a notoriously difficult task. Dozens of different methodologies have been proposed with mixed results, that are not always reproducible. One of the key aspects that is often ignored is the fact that interictally the EEG signals, and consequently the resulting functional brain networks, are far from constant. This observation suggests that seizure detection or prediction algorithms should take into consideration what is the expected value of the EEG signal or of a summary property of the functional brain network at any given time, so that values that differ significantly from this expected value may indicate a seizure.

In this work, we examined how the functional brain networks obtained from scalp EEG measurements evolve in long duration data ranging between 22 and 94 hours. These brain networks were constructed using three different correlation measures - cross-correlation, corrected cross-correlation and coherence - and were then each monitored through three summary network properties: average node degree, global efficiency and average node clustering coefficient. For all three correlation measures, the network properties fluctuated in various repeating cycles that coexist, such as cycles of duration 3, 5, 12 and 24 hours. The most prominent of these is the 24hour cycle that is attributed to the well-known circadian rhythm, where during sleep the network is significantly more connected and clustered in comparison to the duration of wakefulness. The circadian rhythm has been repeatedly shown to occur in the scalp EEG (see, for example, (Kreuz et al. 2004; Schad et al. 2008)), however it is the first time that it is revealed in the long-duration course of the functional brain network obtained from scalp EEG recordings. It could be claimed that periodicity in the above-mentioned summary properties of the network do not necessarily prove periodicity in the functional connections comprising the networks themselves per se; for example, two networks with the same average degree do not necessarily have the same structure. Hence, in order to confirm that the network itself repeats in cycles, we monitored the course of the networks in terms of the structure of their connections (nodes did not change), by means of the graph edit distance measure (Dickinson et al. 2003). The results revealed the same patterns of periodicity in the structure of network connections that we observed for the aforementioned network properties.

Also, we examined the correlation of the periodic characteristics of long-term properties of functional brain networks as quantified by the network average degree and their correlation to seizure onset. Furthermore, we examined the correlation of the periodic

characteristics of signal power and its correlation to seizure onset. Specifically, we examined the correlation of the circadian and smaller periodicities, possibly subharmonics, such as 3.6, 5.4 and 12 hours with the seizure onset. We showed that the periodicities (extracted from the degree) in these networks over different time scales are correlated with seizure occurrence (Figure 8). The instantaneous phases of the main periodic components at seizure onset are not distributed uniformly around the unit circle (Table 4). Instead, especially for the 3.6 and 5.4 hour components, seizures occur within specific phase ranges. We observed that these smaller periodicities obtained from the power in the case of patients with generalized epilepsy were more concentrated around the mean direction in contrast with the focal onset. In contrast, the same periodicities extracted from signal power were uniformly distributed around unit circle indicates that are not significant correlated with seizure (Figure 8). The smaller periodicities were discovered that were harmonics of a longer more prominent periodicity the 24hr. However, from the Figure 8 it seems that the correlation of the periods extracted from the degree with the seizure due to the network itself. Moreover, we showed that the groups were not uniformly distributed around the circle for each instantaneous phase separately (Table 4). In turn, this implies that in order to achieve more reliable seizure detection/prediction, it would be beneficial to include information about the state of these periodicities which also highlights the usefulness of collecting long-term EEG data.

We also examined the occurrence of seizures and how these affected the underlying network, in the long-duration data. Surprisingly, although at smaller scales (several minutes before and after the event) a seizure appears to change the connectivity of the network, when viewed at large (multi-hour/day) scale, this effect is subtle in comparison to the changes due to the intrinsic periodicity of the networks. Hence, seizure detection or prediction based solely on whether some network properties obtain values larger than a constant, prespecified threshold do not suffice and are expected to yield either many false positives - if the threshold if relatively low - or many false negatives - if it is relatively high.

In 2010, Kuhnert et al. conducted a study similar to ours, on the predictability of epilepsy from long-duration EEG data. They recorded intracranial EEG data and constructed functional brain networks using mean phase coherence as the measure of node correlation; the weighted networks were then binarize by setting a threshold that keeps the mean degree constant across consecutive windows. The authors monitored how the characteristic path length and the clustering coefficient changed over time. Despite all the differences in the construction of the functional brain networks - in the type of recording (intracranial vs scalp), in the montage used (reference vs bipolar), in the correlation measure (mean phase coherence vs cross-

correlation, corrected cross-correlation, and coherence) and in the method of binarization (varying threshold to keep mean degree constant vs constant threshold) - our results confirm what was shown by Kuhnert et al., in 2010: first, that the functional brain networks change periodically over time, with the most prominent cycle of approximately 24 hours, and second, that seizures influence the brain networks significantly less than the daily rhythms. In 2015, Geier et al. investigated the long-term evolution of degree-degree correlations (assortativity) in functional brain networks from epilepsy patients. They recorded intracranial EEG data and they followed the procedure described in Kuhnert et al. (2010) for the construction of the functional networks. The authors monitored how the assortativity and the clustering coefficient changed over time. Again with this study despite all the differences, our results confirm what was shown by Geier et al. in 2015: first, that large fluctuations in time-resolved degree-degree correlations ranging from assortative to dissortative mixing, exhibiting some periodic temporal structure which can be attributed, to a large extent, to daily rhythms, and second, relevant aspects of the epileptic process, particularly possible pre-seizure alterations, contribute marginally to the observed long-term fluctuations. In 2017, Geier and Lehnertz investigated the temporal and spatial variability of the importance regions in evolving epileptic brain networks. Specifically, as described in Kuhnert et al. (2010), by using intracranial EEG recordings they constructed functional brain networks using mean phase coherence as the measure of node correlation and use strength and betweenness centrality in order to investigate the importance of brain regions (Geier and Lehnertz 2017). The authors observed the importance of brain regions to fluctuate over time with these fluctuations were mostly attributed to processes acting on timescales of hours to days, with strong contribution to daily rhythms. Our results are similar in some extent proving that there are some periodic fluctuations that can be attributed to phenomena related to the disease.

The added value of this work -apart from confirming the results of Kuhnert et al. (2010), Geier et al. (2015) and Geier and Lehnertz (2017) using different methodology for recording the EEG and for constructing the functional brain networks-is twofold. First, we presented a novel way to calculate network topologies based on the measure of graph edit distance, and based on that we proved that the functional brain network itself, and not just some summarizing properties (such as the clustering coefficient) repeats periodically. Second, we also showed that in addition to the circadian, 24-hour cycle, there co-exist many more cycles that are clearly reflected in the functional brain network. Also, we observed that periodicity of 24hr and shortest periodicities such as 12hr, 5.4hr and 3.5hr, are correlated with seizure onset. Specifically, the network-based periodicities are much more synchronized to seizures than

EEG signal power itself. Moreover, with the methodology applied in this work, the periodic fluctuations, especially the circadian ones, are much more clearly visible even by naked eye (compare for example Figure 2 in this chapter with Figure 1 in (Kuhnert et al. 2010).

Acknowledgements

This work was partially supported by the European Regional Development Fund and the Republic of Cyprus through the Research Promotion Foundation (Project ΥΓΕΙΑ/ΔΥΓΕΙΑ/0609(ΒΕ)/11).

References

Bazil CW, Walczak TS. Effects of sleep and sleep stage on epileptic and nonepileptic seizures. Epilepsia. 1997;38(1):56–62.

Berens P. CircStat : A MATLAB Toolbox for Circular Statistics. J Stat Softw. 2009;31(10):1–21.

Bruzzo AA, Gesierich B, Santi M, Tassinari CA, Birbaumer N, Rubboli G. Permutation entropy to detect vigilance changes and preictal states from scalp EEG in epileptic patients. A preliminary study. Neurol Sci. 2008;29(1):3–9.

Burns SP, Santaniello S, Yaffe RB, Jouny CC, Crone NE. Network dynamics of the brain and influence of the epileptic seizure onset zone. Proc Natl Acad Sci U S A. 2014;111(49):E5321-5330.

Chapotot F, Jouny C, Muzet A, Buguet A, Brandenberger G. High frequency waking EEG: reflection of a slow ultradian rhythm in daytime arousal. Neuroreport. 2000;11(10):2223–7.

Christodoulakis M, Hadjipapas A, Papathanasiou E, Anastasiadou M, Papacostas S, Mitsis G. On the Effect of Volume Conduction on Graph Theoretic Measures of Brain Networks in Epilepsy. In: Sakkalis V, editor. Modern Electroencephalographic Assessment Techniques. Springer New York; 2015. p. 103–30. (Neuromethods; vol. 91).

Daly I, Nicolaou N, Nasuto SJ, Warwick K. Automated Artifact Removal From the Electroencephalogram: A Comparative Study. Clin EEG Neurosci. 2013;44(4):291–306.

Dickinson PJ, Bunke H, Dadej A, Kraetzl M. On Graphs with Unique Node Labels. In: Hancock E, Vento M, editors. Graph Based Representations in Pattern Recognition. Springer Berlin Heidelberg; 2003. p. 13–23. (Lecture Notes in Computer Science; vol. 2726).

Ferri R, Rundo F, Bruni O, Terzano MG, Stam CJ. Small-world network organization of functional connectivity of EEG slow-wave activity during sleep. Clin Neurophysiol. 2007;118(2):449–56.

Ferri R, Rundo F, Bruni O, Terzano MG, Stam CJ. The functional connectivity of different EEG bands moves towards small-world network organization during sleep. Clin Neurophysiol. 2008;119(9):2026–36.

Fisher NI. Statistical Analysis of Circular Data:. Cambridge: Cambridge University Press; 1993.

Geier C, Bialonski S, Elger CE, Lehnertz K. How important is the seizure onset zone for

seizure dynamics'. Seizure. 2015a;25:160–6.

Geier C, Kuhnert MT, Elger CE, Lehnertz K. On the centrality of the focus in human epileptic brain networks. Recent Adv Predict Prev Epileptic Seizures. 2013;(2013):175–85.

Geier C, Lehnertz K. Long-term variability of importance of brain regions in evolving epileptic brain networks. Chaos An Interdiscip J Nonlinear Sci. 2017 Apr 1;27(4):43112.

Geier C, Lehnertz K, Bialonski S. Time-dependent degree-degree correlations in epileptic brain networks: from assortative to dissortative mixing. Front Hum Neurosci. 2015b;9(August):462.

Kaiser DA. Ultradian and circadian effects in electroencephalography activity. Biofeedback. 2008;36(4):148.

Kaiser DA, Sterman MB. Periodicity of Standardized EEG Spectral Measures across the Waking Day. In: 7th Annual Summer Sleep Workshop Multi-Site Training Program for Basic Sleep Research. Lake Arrowhead, California; 1994.

Klingspor M. Hilbert Transform : Mathematical Theory and Applications to Signal processing. Linköping University, Faculty of Science and Engineering; 2015. (LiTH-MAT-EX).

Koschützki D, Lehmann KA, Peeters L, Richter S, Tenfelde-Podehl D, Zlotowski O. Centrality Indices. In: Network analysis. 2005. p. 16–61.

Kramer MA, Eden UT, Lepage KQ, Kolaczyk ED, Bianchi MT, Cash SS. Emergence of persistent networks in long-term intracranial EEG recordings. J Neurosci. 2011;31(44):15757–67.

Kramer MA, Kolaczyk ED, Kirsch HE. Emergent network topology at seizure onset in humans. Epilepsy Res. 2008;79(2--3):173–86.

Kreuz T, Andrzejak R, Mormann F, Kraskov A, Stögbauer H, Elger CE, et al. Measure profile surrogates: A method to validate the performance of epileptic seizure prediction algorithms. Phys Rev E. 2004;69(6):61915.

Kuhnert M-T, Elger CE, Lehnertz K. Long-term variability of global statistical properties of epileptic brain networks. Chaos An Interdiscip J Nonlinear Sci. 2010;20(4):43126.

Latora V, Marchiori M. Efficient behavior of small-world networks. Phys Rev Lett. 2001 Nov;87(19):198701.

Lehnertz K, Ansmann G, Bialonski S, Dickten H, Geier C, Porz S. Evolving networks in the human epileptic brain. Phys D Nonlinear Phenom. 2014;267:7–15.

Mathworks. Find Periodicity Using Autocorrelation. 2015.

Minecan D, Natarajan A, Marzec M, Malow B. Relationship of epileptic seizures to sleep stage and sleep depth. Sleep. 2002;25(8):899–904.

Navarro V, Martinerie J, Le Van Quyen M, Baulac M, Dubeau F, Gotman J. Seizure anticipation: Do mathematical measures correlate with video-EEGevaluation? Epilepsia. 2005;46(3):385–96.

Nevado A, Hadjipapas A, Kinsey K, Moratti S, Barnes GR, Holliday IE, et al. Estimation of functional connectivity from electromagnetic signals and the amount of empirical data required. Neurosci Lett. 2012 Mar 28 [cited 2013 Mar 25];513(1):57–61.

Nicolaou N, Nasuto SJ. Comparison of Temporal and Standard Independent Component Analysis (ICA) Algorithms for EEG Analysis. In: In: Tenth international conference on neural information processing (ICANN/ICONIP'03). 2003. p. 157–60.

Nicolaou N, Nasuto SJ. Automatic Artefact Removal from Event-related Potentials via Clustering. J VLSI Signal Process Syst Signal Image Video Technol. 2007;48(1):173–83.

Rubinov M, Sporns O. Complex network measures of brain connectivity: uses and interpretations. Neuroimage. 2010 Sep [cited 2013 Feb 11];52(3):1059–69.

Schad A, Schindler K, Schelter B, Maiwald T, Brandt A, Timmer J, et al. Application of a multivariate seizure detection and prediction method to non-invasive and intracranial long-term EEG recordings. Clin Neurophysiol. 2008;119(1):197–211.

Scheich H. Interval histograms and periodic diurnal changes of human alpha rhythms. Electroencephalogr Clin Neurophysiol. 1969;26(4):442.

Schelter B, Feldwisch-Drentrup H, Ihle M, Schulze-Bonhage A, Timmer J. Seizure Prediction in Epilepsy: From Circadian Concepts via Probabilistic Forecasting to Statistical Evaluation. In: 2011 Annual International Conference of the IEEE Engineering in Medicine and Biology Society. 2011. p. 1624–7.

Schelter B, Winterhalder M, Maiwald T, Brandt A, Schad A, Timmer J, et al. Do false predictions of seizures depend on the state of vigilance? {A} report from two seizure-prediction methods and proposed remedies. Epilepsia. 2006;47(12):2058–70.

Terzano MG, Mancia D, Salati MR, Costani G, others. The cyclic alternating pattern as a physiologic component of normal {NREM} sleep. Sleep J Sleep Res Sleep Med. 1985;

Terzano MG, Parrino L, Spaggiari MC. The cyclic alternating pattern sequences in the dynamic organization of sleep. Electroencephalogr Clin Neurophysiol. 1988;69(5):437–47.

Theiler J, Eubank S, Longtin A, Galdrikian B, Farmer JD. Testing for nonlinarity in time series: the method of surrogate data. Phys D. 1992;58(1–4):77–94.

Varotto G, Tassi L, Franceschetti S, Spreafico R, Panzica F. Epileptogenic networks of type II focal cortical dysplasia: A stereo-EEG study. Neuroimage. 2012;61(3):591–8.

Watts DJ, Strogatz SH. Collective dynamics of "small-world" networks. Nature. 1998 Jun;393(6684):440–2.

Wilke C, Worrell G, He B. Graph analysis of epileptogenic networks in human partial epilepsy. Epilepsia. 2011;52(1):84–93.

Zar JH. Biostatistical Analysis. Prentice Hall; 1999.

Ziehe A, Müller K-R. TDSEP --- an efficient algorithm for blind separation using time structure. In: Niklasson L, Bodén M, Ziemke T, editors. ICANN 98: Proceedings of the 8th International Conference on Artificial Neural Networks, Skövde, Sweden, 2--4 September 1998. London: Springer London; 1998. p. 675–80.

Zubler F, Gast H, Abela E, Rummel C, Hauf M, Wiest R, et al. Detecting Functional Hubs of Ictogenic Networks. Brain Topogr. 2014;28(2):305–17.